

Time and frequency domain solutions in an optical analogue of Grover's search algorithm

T.W. Hijmans, T.N. Huussen, and R.J.C. Spreeuw

*Van der Waals-Zeeman Instituut, Universiteit van Amsterdam,
Valckenierstraat 65, 1018 XE, Amsterdam, The Netherlands.**

(Dated: July 18, 2018)

We present new results on an optical implementation of Grover's quantum search algorithm. This extends previous work in which the transverse spatial mode of a light beam oscillates between a broad initial input shape and a highly localized spike, which reveals the position of the tagged item. The spike reaches its maximum intensity after $\sim \sqrt{N}$ round trips in a cavity equipped with two phase plates, where N is the ratio of the surface area of the original beam and the area of the phase spot or tagged item. In our redesigned experiment the search space is now two-dimensional. In the time domain we demonstrate for the first time a multiple item search where the items appear directly as bright spots on the images of a gated camera. In a complementary experiment we investigate the searching cavity in the frequency domain. The oscillatory nature of the search algorithm can be seen as a splitting of cavity eigenmodes, each of which concentrates up to 50% of its power in the bright spot corresponding to the solution.

© 2018 Optical Society of America

OCIS codes: 070.2580, 200.3050, 030.1670

*Electronic address: hijmans@science.uva.nl

1. Introduction

Of all algorithms proposed for implementation on quantum computers, Grover's search algorithm^{1,2} is perhaps the most successful in terms of experimental demonstrations. The algorithm has been successfully tested in a variety of experiments, ranging from NMR to purely optical realizations^{3,4,5,6,7,8,9}. The algorithm performs the following task: given a random list of N items, one of which is labeled, it seeks out the tagged item in $O(\sqrt{N})$ computational steps. A classical search, based on randomly testing items until the desired tagged one is found, requires on average $\frac{1}{2}N$ tries. Hence for large N the Grover quantum algorithm leads to a quadratic speedup of the search procedure compared to classical methods.

Whereas in general quantum interference and entanglement are considered essential for quantum computation, it has been shown that entanglement is not essential for quantum searching and that it is possible to implement Grover's algorithm relying only on interference¹⁰. It has been demonstrated experimentally that one can construct a purely optical method using classical light that closely follows Grover's original quantum algorithm⁸. The underlying mapping is sometimes called a "unary" representation. There remains one essential difference between the classical implementation and the true quantum algorithm: the resources (essentially the minimal size of the apparatus) needed for the unary version scale linearly with N whereas the resources for the quantum version scale only as $\log N$. Indeed, with this proviso, the unary mapping allows the implementation of any quantum algorithm for small numbers of qubits, even in the presence of entanglement^{11,12}.

In this paper we experimentally investigate an optical, unary, implementation of Grover's search algorithm that differs in one essential aspect from previous versions. As usual, the output of the device oscillates between a standard input and the sought solution. The period of the oscillation is approximately $(\pi/2)\sqrt{N}$. After one half period the output coincides exactly with the sought solution.

The oscillatory nature of the output in Grover's algorithm closely resembles a Rabi oscillation of a two level atom, the role of the two levels being taken over by the states corresponding to the standard input and the solution, respectively. The fact that effectively only two states participate, suggests that it is possible to bring the system into a steady state consisting of a superposition of the input state and the sought solution.

In the present experiment we compare two versions of implementing Grover's algorithm.

The first version we use a pulse of light and observe oscillation of the transverse mode between a broad standard input shape and a narrow spike, which corresponds to the solution of the search problem. In the second version we use a single frequency light source and exploit the resonant properties of a Fabry-Perot type cavity into which the Grover iterator has been embedded, to construct the aforementioned superposition state of input state and solution.

Our optical implementation is similar to the one that was published previously⁸, but has been modified in several essential ways. The original experiment has been redesigned completely, now using a two-dimensional search space instead of a one-dimensional one, and a gated camera to selectively look at the entire beam profile after a chosen number of cavity round trips. The size of the search space in the present experiment ranges between about 400 to 1000 items, depending on the conditions chosen, and allowed us to demonstrate for the first time a multiple item search. The tagged items appear directly as bright spots in the camera images. In a complementary experiment we feed the cavity with monochromatic light and scan the cavity, observing Fabry-Perot resonances that are modified by the search.

The remainder of this paper is organized as follows: In the next section we describe the principle of the experiment and its interpretation. In section 3 we present the experimental details, and in sections 4 and 5 we present results for the pulsed and cw versions of the experiment, respectively. Finally, we discuss these results in section 6.

2. Principle of the experiment

In its quantum implementation Grover's algorithm starts out with an n -qubit string which is prepared in a uniform superposition of all its $2^n \equiv N$ states. A quantum operation called Grover's iterator is then applied repeatedly to the n -qubit string. This operation does the following: first the amplitude of a single tagged state, which is unknown at the outset, is inverted. The second step is an inversion of all amplitudes about their average value. By repeating the Grover iterator $\sim \sqrt{N}$ times the state is gradually transformed from the uniform superposition into purely the tagged state: we have found our solution.

The quantum algorithm has the following classical, unary, analog. The search space is defined as the cross sectional area of a coherent light beam of effective radius R_b . Let us divide the transverse mode profile of this beam into N small sections. The complex field amplitudes of the transverse beam profile in these N sections represent the state vector. We tag one of these sections by sending the beam through a phase plate, called the "oracle",

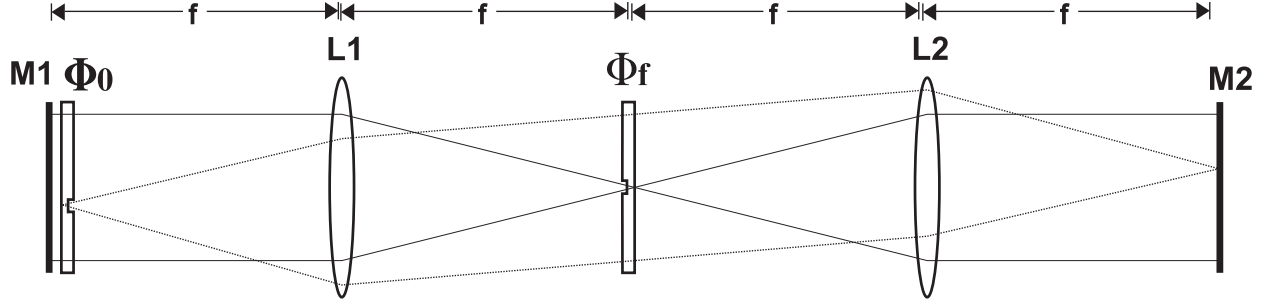


Fig. 1. Optical cavity implementing the Grover iterator. M1: input mirror, M2: output mirror, L1, L2: lenses, Φ_0 : oracle phase-plate, Φ_f : focus phase-plate

that contains a small circular spot that locally changes the phase of the beam by $\pi/2$. It is natural to define the size of the search space as $N = (R_b/r_s)^2$ where r_s is the radius of the phase spot. The phase spot is placed in an arbitrary transverse position within the beam profile. The task at hand is to identify the location of this phase spot in as few steps as possible. This is done by passing the beam repeatedly through a setup that has the property to progressively transfer more and more intensity to the position of the phase spot. As soon as all light intensity is concentrated in the spot we have found our solution.

In Fig. 1 we show the heart of the experimental setup. It consists of a linear cavity with two mirrors with a reflectivity of 90%. Inside the cavity there are two lenses of focal length $f = 0.34$ m, equal to $1/4$ of the cavity length. The lenses are positioned at a relative distance of $2f$ and symmetric relative to the center of the cavity. The oracle phase plate is positioned as close as possible to the input mirror of the cavity and can be translated in two directions perpendicular to the beam axis to ensure that the phase spot can be positioned arbitrarily inside the beam profile. A second phase plate is positioned at the common focus of the two lenses, in the center of the cavity. Like the oracle, this phase plate contains a small disk-shaped area in which the phase of the light wave is changed by $\pi/2$. The size of the phase spots in both phase plates is chosen equal to the waist of the light beam at the common focus of the two lenses. The lenses and mirror are located such that the transverse mode profile at the input mirror and oracle, and that at the focus phase plate, are each others Fourier transform. It is this property that makes this setup perform the equivalent of Grover's algorithm. Each round trip both phase plates are passed twice, leading to a local phase shift of π per round trip. In Table 1 we show the correspondence between the operations of the quantum algorithm and its classical unary equivalent.

Quantum	Classical
1. Oracle $I - 2 s\rangle\langle s $	$\Phi_0^2 = \exp[2i\phi(x, y)]$
2. Hadamard $H^{\otimes n}$	\mathcal{F}
3. $I - 2 0\rangle\langle 0 $	$\Phi_f^2 = \exp[2i\varphi(x, y)]$
4. Hadamard $H^{\otimes n}$	\mathcal{F}^{-1}

Table 1. Comparison of quantum and classical operators in the search protocol. Steps 2 through 4 in the quantum version are the ‘inversion about average’ (IAA) operation, \mathcal{F} denotes Fourier transformation. ϕ and φ denote the phase shifts imparted by the oracle and focus phase plate, respectively. The factor 2 inside the exponent appears because the setup is used in double pass.

In the notation of Table 1 we obtain the following expression for the classical implementation of the Grover iterator:

$$\mathbf{G} = \Phi_0^2 \mathcal{F}^{-1} \Phi_f^2 \mathcal{F}. \quad (1)$$

Here the squares reflect the fact that the experiment uses a double pass of each phase plate every round trip.

The normalized form of an intensity at position \mathbf{r} which is nonzero only in the circular region of one of the phase plates is given as:

$$I_1(\mathbf{r}) = \frac{1}{\pi r_s^2} \theta(r_s - |\mathbf{r} - \mathbf{r}_i|), \quad (2)$$

where θ is the unit step function and \mathbf{r}_i is the location of the center of the phase spot. On the focus plate $\mathbf{r}_i = 0$, on the oracle it is the arbitrary position which we wish to find.

In the experiment we use a Gaussian input beam. Unfortunately the Fourier transform of a Gaussian does not exactly match the shape of the circular focus phase spot. Therefore, in the theoretical analysis of the experiment we will assume that the input beam has the intensity profile of an Airy disk given in a form normalized to unity when integrated over the radial coordinates by:

$$I_0(r) = \frac{kr_s}{4\pi f^2} \left[\frac{2J_1(\rho)}{\rho} \right]^2, \quad (3)$$

where $\rho = kr_s r/f$, with k , r , and f , respectively denoting the wave vector of the light, the distance from the center in the input beam and the focal length of the lenses. The number

of channels is given as

$$N = 4f^2/k^2r_s^4. \quad (4)$$

The amplitude corresponding to I_0 takes the role of the uniform superposition of all possible n -bit strings used as input to Grover's algorithm and the amplitude corresponding to I_1 takes the role of the solution. Without loss of generality we can choose these amplitudes $\psi_0(\mathbf{r})$ and $\psi_1(\mathbf{r}, \mathbf{r}_i)$ to be real. We can define the overlap of these amplitude functions as:

$$\chi(\mathbf{r}_i) = \int_{-\infty}^{\infty} \int_{-\infty}^{\infty} \psi_0(\mathbf{r}) \psi_1(\mathbf{r}, \mathbf{r}_i) d^2\mathbf{r}. \quad (5)$$

The two functions ψ_0 and ψ_1 are almost but not quite orthonormal. If \mathbf{r}_i is chosen within the central disk of the Airy pattern the overlap integral is of order $1/\sqrt{N}$. It is useful to orthonormalize the two functions by retaining ψ_1 and defining

$$\tilde{\psi}_0(\mathbf{r}) = \frac{1}{\sqrt{1-\chi^2}} [\psi_0(\mathbf{r}) - \chi(\mathbf{r}_i) \psi_1(\mathbf{r}, \mathbf{r}_i)] \quad (6)$$

We will now analyze the action of the setup of Fig. 1 for several cases using the above definitions. We will first assume that the reflectivity of the mirrors is unity and that additional losses are absent. When a light pulse performs a complete round trip through the cavity each phase plate locally imparts a $\pi/2$ phase change twice. One can show that a setup where the phase plates impart a phase change of π only once is equivalent apart from trivial overall phase factors. Experimentally this could be realized by using a ring cavity rather than a linear one. We will adopt this assumption, which also is implicit in Eq. (1), to slightly simplify the analysis.

Using the two orthonormal amplitude functions $\tilde{\psi}_0$ and ψ_1 , one can easily show they transform in the following manner after a single round trip of the cavity, up to an overall phase factor depending on the cavity length:

$$\tilde{\psi}_0 \rightarrow \tilde{\psi}_0(1 - 2\chi^2) + 2\chi\psi_1 \quad (7)$$

$$\psi_1 \rightarrow \psi_1(1 - 2\chi^2) - 2\chi\tilde{\psi}_0, \quad (8)$$

where we have suppressed the explicit dependence on the radial coordinates. Eqs. (7,8) are an approximation, valid up to second order in χ . It is derived by propagating the amplitudes $\tilde{\psi}_0$ and ψ_1 through the setup, imparting a phase shift of π to the part of each function at the position of the phase spots once each round trip.

If we start with all the power in the mode $\tilde{\psi}_0$, the relative power in the two above modes at subsequent time τ is expressed as the diagonal elements ρ_{00} and ρ_{11} which, to second order in χ , take the form: $\rho_{00} = \cos^2(2\chi\tau)$ and $\rho_{11} = \sin^2(2\chi\tau)$. Here the time τ is measured in units of cavity round trip time. This time dependence is analogous to a Rabi oscillation in an undamped two level atom, which reflects the well known fact that in Grover's search problem the evolution is limited to a two level subspace.

Note that the overlap χ actually depends on the relative distance \mathbf{r}_i of the oracle to the beam axis. If the oracle approaches the origin the overlap becomes equal to $\chi = 1/\sqrt{N}$. In this case the amplitude of the solution is maximum for $\tau = \pi\sqrt{N}/4$, corresponding to Grover's solution. If the oracle is placed further outward, the search time increases slightly, to become infinite for the oracle approaching a distance equal to the first dark ring in the Airy disk.

The experiments described in the next section fall in two categories. In the first experiment we proceed essentially as just outlined, a small portion of the intensity of a short pulse is admitted to the cavity through a mirror with high, but finite reflectivity, in a beam profile closely resembling that of Eq. (3). After each successive round trip the mode evolves towards the sought solution. In a second category of experiments we use cw light and look at the steady state solution of the transverse mode in the cavity. We will assume that the cavity is continually being fed light in mode ψ_0 through an input mirror with amplitude transmission coefficient t . In the cavity we assume that the transverse mode at the position of the mirror, is given by $a_0\tilde{\psi}_0 + a_1\psi_1$. The losses of the cavity are taken into account by assuming that they are entirely due to the finite mirror reflectivity which leads to a reduction of the amplitudes by a factor $\sqrt{1-t^2}$ for each of the two mirrors of the cavity. The variable cavity length introduces an overall phase factor $\exp[i\alpha]$ after each round trip for both amplitudes. Experimentally this phase factor can be varied either by sweeping the frequency of the light source or by varying the cavity length. The condition of steady state then leads, in analogy to Eq. (8), to the following equations:

$$a_0 = \{a_0(1 - 2\chi^2) - 2\chi a_1\}(1 - t^2) \exp[i\alpha] + t \quad (9)$$

$$a_1 = \{a_1(1 - 2\chi^2) + 2\chi a_0\}(1 - t^2) \exp[i\alpha], \quad (10)$$

where the input power has been normalized to unity.

The solution of these equations is plotted in Fig. 2 for $\chi = 0.05$. This corresponds to a

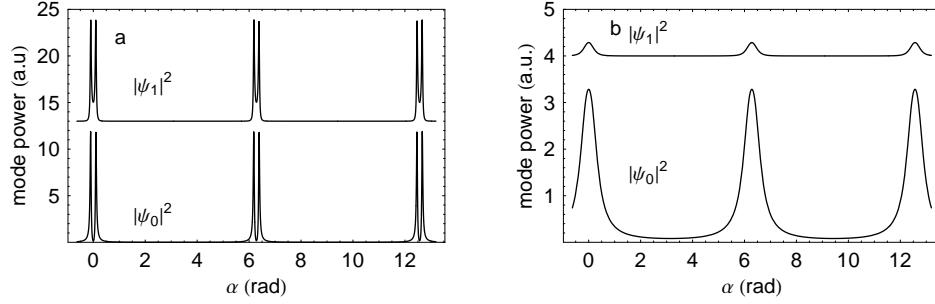


Fig. 2. Calculation of the power corresponding to the eigenmodes plotted versus the cavity phase shift angle α , of a cavity with an oracle and a focus phase plate inserted, each imparting a local phase shift of π each round trip. The lower trace in each figure corresponds to the mode $\tilde{\psi}_0$, the upper trace to ψ_1 . The traces for ψ_1 have been translated upwards for visual clarity. In both figures $\chi = 0.05$. The a and b panels correspond to $t = 0.15$ (a Finesse F of 138), and $t = 0.5$ ($F = 9$), respectively.

value of $N = 400$ a number roughly corresponding to the experimental conditions below. In the figure we plot the calculated power inside the cavity for both modes, as a function of the round-trip phase shift. The result for both modes is similar to the normal behavior for a resonant cavity, showing sharp maxima when the effective cavity length is an integer number of half wavelengths. However, on close inspection the resonance maxima are doublets with a splitting that scales with χ . The two lines of the doublet are only resolved if the finesse F of the cavity is of the order of or bigger than π/χ . For a two mirror Fabry-Perot type cavity this finesse given by $F = \pi\sqrt{R}/(1 - R)$ where $R = 1 - t^2$.

What we see from Fig. 2 is that as soon as the finesse of the cavity is sufficiently large, the transverse mode is a doublet corresponding to the superpositions $\frac{1}{\sqrt{2}}(\tilde{\psi}_0 \pm \psi_1)$. Almost half the power is found in the solution ψ_1 , for both components of the doublet. In this doublet-resolved (“good cavity”) limit, the intensity of the solution, on resonance, is a factor N higher than in the background, i.e. in other positions.

At this point it is instructive to consider the resource requirements. We could imagine setting the cavity on one of the doublet resonances and injecting a very low intensity, with on average a single photon inside the cavity. Since F is essentially the number of roundtrips inside the cavity, and $F > \pi/\chi \sim \sqrt{N}$, this single photon will be detected after a time $O(\sqrt{N})$. As this photon has 50% probability to be detected in the solution, only a small, fixed number of repetitions is needed. The usual \sqrt{N} quantum search efficiency thus appears

here as a temporal resource requirement.

In the opposite limit $F \ll \sqrt{N}$, where the doublet is unresolved, the quadratic speedup is lost. One can easily show that the contrast between the solution and the background becomes $\sim F^2 \ll N$. Note however that for a realistic finesse the contrast can still be substantially larger than unity. The setup can be thus be seen as a phase contrast microscope with a contrast enhanced by several orders of magnitude. This may have applications beyond quantum information processing.

3. Experimental details

The input light to the cavity comes from a 656 nm diode laser. The laser in the pulsed experiment emits sub-ns pulses with a repetition rate of 40 MHz, in the cw experiment we use a grating stabilized laser to obtain single frequency cw light. The light is coupled into an optical fiber to obtain a Gaussian TEM₀₀ beam profile. To implement the phase shift of $\pi/2$, the phase plates consist of a fused silica substrate with a dimple that is 359 nm deep (note that a bump instead of a dimple would work as well). Phase plates of different diameters ranging from 63 to 127 μm were used. From Eq. (4) we find that this corresponds to a number of channels ranging from 300 to well over 1000. In most experiments the effective channel number was about 400. The input beam has a Gaussian shape which approximately matches the central lobe of the Airy disc of the ideal case discussed in the previous section. For phase spots of 100 μm diameter the half width of this Gaussian beam is about 2.5 mm. The exact beam diameter was optimized empirically in the experiment depending on which phase plates were used.

The phase plates were manufactured using photolithography and plasma etching. For technical reasons we decided to make holes instead of bumps. The measured depth of the etched surfaces is about 344 nm with a non-uniformity of at most 14 nm. The corresponding phase shift is 1.51 ± 0.06 rad, which deviates less than 8% from the ideal $\pi/2$ value. In order to minimize optical losses a multi-layer coating was applied to the phase plates, reducing the reflectivity to less than 0.25%.

In the 1D version of the pulsed experiment Bhattacharya et al.⁸ used a single photodiode for detection of the output signal. The aim of our setup is to obtain a full 2D picture of the search result. A CCD camera is suitable for this purpose, but it is too slow to distinguish the pulses coming out of the cavity, spaced in time by about 10 ns. Therefore we implemented

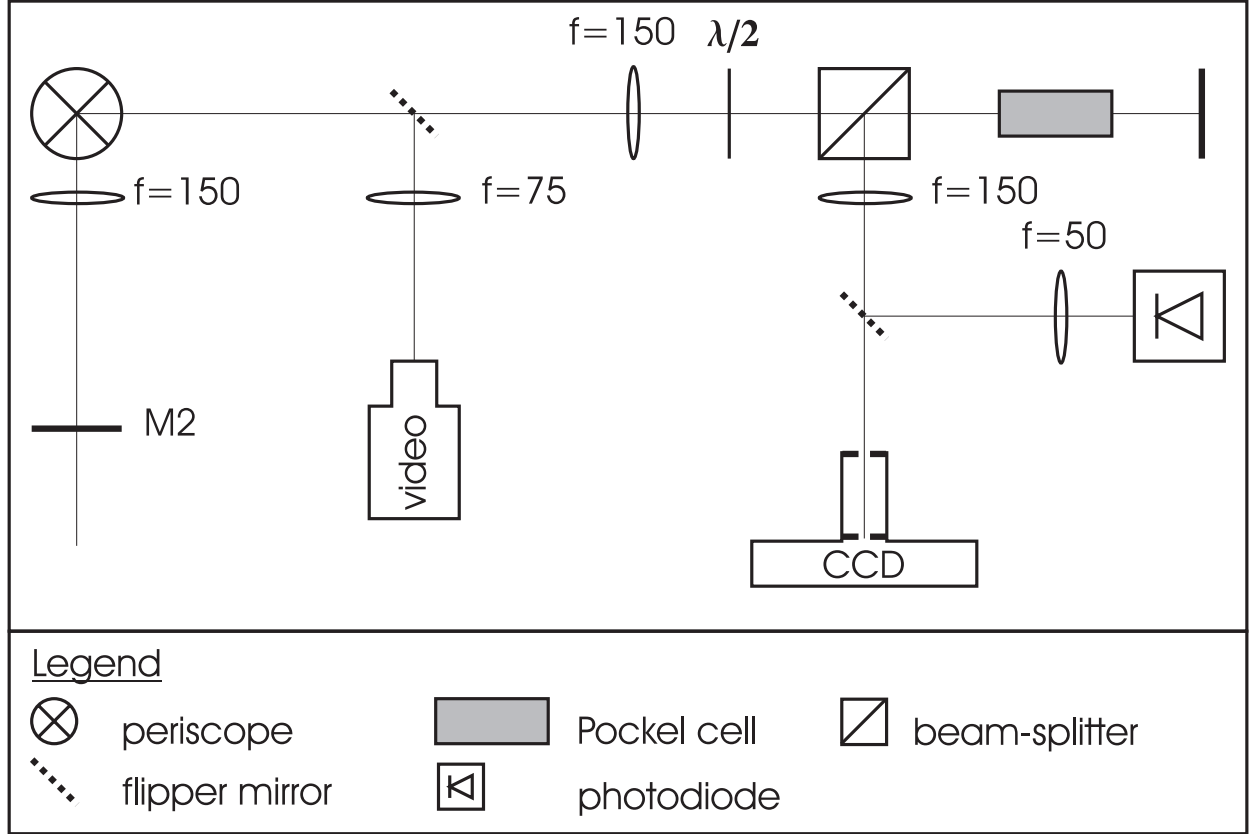


Fig. 3. Setup for imaging. The image at mirror M2 is relayed and imaged onto the CCD camera. The half-wave plate rotates the polarization such that all light passes through the polarizing beam-splitter to the Pockels-cell. We use the Pockels-cell in double-pass configuration to obtain an effective retardation of $\lambda/2$, such that the retro-reflection is completely reflected by the beam-splitter. The last lens images the search result on the CCD-chip, or the photodiode. The light path can be diverted to a video camera for real time monitoring of the image on the output mirror, used in the CW experiment. In these experiments the video camera is replaced, after alignment, by a photo diode behind a $150\mu\text{m}$ aperture.

a setup for fast optical gating using a Pockels cell. The layout of the imaging part of the setup is shown in Fig. 3. The fast gate allows us to select a single pulse from the pulse train that leaves the cavity. Each pulse corresponds to $(i - \frac{1}{2})$ iterations ($i = 1, 2, 3, \dots$) of the search algorithm. We are able to select i -th pulse in repetitive measurements, such that we can integrate the image on the camera. The high voltage supply to the Pockels cell allows for a maximum repetition rate of 250 Hz and an exposure time of about one minute yields

good readout statistics.

In the cw experiments we used a fixed laser frequency and a galvo driven rotating Brewster plate in the cavity to change its effective length to obtain the spectra. The image at the output mirror of the cavity was imaged onto a video camera to obtain a qualitative impression of the spatial mode. For quantitative analysis the camera was replaced by a photodiode with a $150\mu\text{m}$ aperture in front. This photodiode and aperture were mounted on an x-y translation stage allowing the transverse intensity profile to be scanned. In the cw experiments the effective cavity length was scanned over several wavelengths, using the Brewster plate. The typical scan time was a few hundred ms.

4. Results of the time domain experiments

In Fig. 4 we show the result of the pulsed version of the experiment using an oracle containing a $63\mu\text{m}$ diameter dot together with a $90\mu\text{m}$ diameter focus spot. Theoretically the solution would reach a maximum after about 20 iterations. In the figure we show a horizontal slice of the image obtained on the CCD, going through the bright spot. The four images are taken after $\frac{1}{2}$, $1\frac{1}{2}$, $2\frac{1}{2}$, and $3\frac{1}{2}$ round trips, respectively. The shift by half a round trip occurs because the light enters the cavity from the left and the output is imaged on the right mirror (M2) in Fig. 1. It is clearly seen that the ratio of the intensity of the sharp feature to that of the broad background increases significantly with each iteration. In Fig. 4 we have subtracted the light-free background recorded on the CCD. After 4 passes the remnants of the signal corresponding to the input field have dropped below zero due to slow drifts relative to the background signal. The images all have the same scale.

The sharp feature, the solution, does not display the expected linear increase with time. The reason is that the cavity suffers from considerable losses due to the finite transmittance of the mirrors, reflectivity losses at the surfaces of lenses and phase plates, and diffraction losses at the edges of the phase spots, which after all are necessarily imperfectly matched to the Gaussian input beam. The losses can be measured experimentally but we defer a quantitative discussion of this measurement to the next section. Here we can say that the results of Fig. 4 show that the solution reaches its maximum amplitude already after 2 or three round trips which implies that the losses amount to 30 or perhaps even 50% per complete round trip.

Before we turn to the cw results it is worth commenting briefly on a version of Grover's

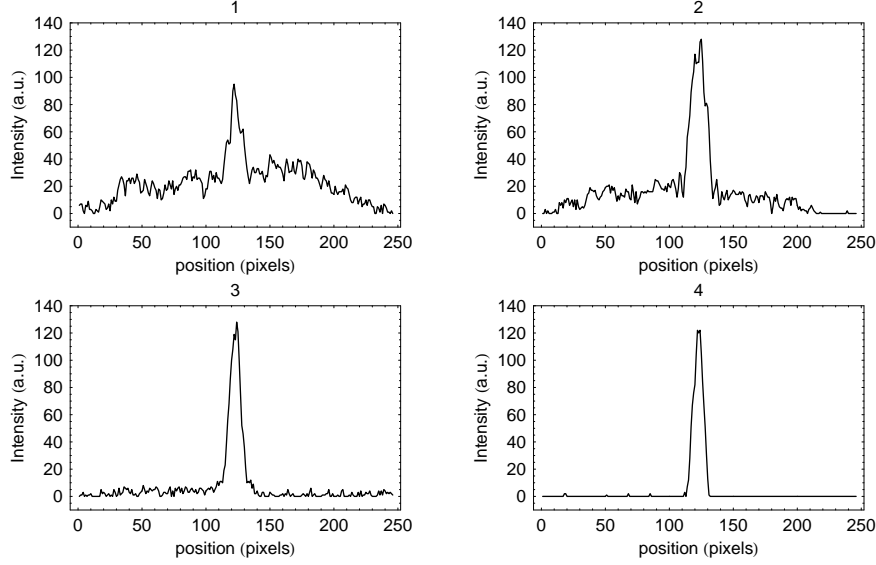


Fig. 4. Cross section through the CCD image after a single pass ($\frac{1}{2}$ round trip) and $1\frac{1}{2}, 2\frac{1}{2}$, and $3\frac{1}{2}$ roundtrips. The images have the same scale and have not been corrected for losses.

algorithm in which $M > 1$ items are tagged. In this case, starting from the same state as in the one item case, a superposition of the M solution states is reached after $O(\sqrt{N/M})$ iterations^{1,2,13}. We have investigated several examples of multi-item searching. A representative example, where we use an oracle with three identical phase spots of $100 \mu\text{m}$ diameter, is shown in Fig. 5. The result is qualitatively similar to the one item case: the contrast between the solutions and the background increases with each iteration while the overall power drops rather quickly due to the losses mentioned above.

5. Results of the frequency domain experiments

As was discussed in section 2, the setup shown in Fig. 1 is in essence a Fabry-Perot (F-P) resonator. By using cw light and scanning the cavity length we can monitor its resonance properties. First we measure the total power transmitted at the output of the cavity with the phase plates positioned such that both phase spots are completely outside the beam profile. The result is the upper trace (a) shown in Fig. 6. The characteristic peak structure of the F-P resonator is visible. From this trace we find a finesse F of about 20. If this were entirely due to the mirror reflectivity we would infer $R = 0.85$. In reality we use mirrors with $R = 0.90$. The rather low F is consistent with this value of R combined with the losses of approximately 0.25% per surface of the two lenses, the phase plates and the Brewster

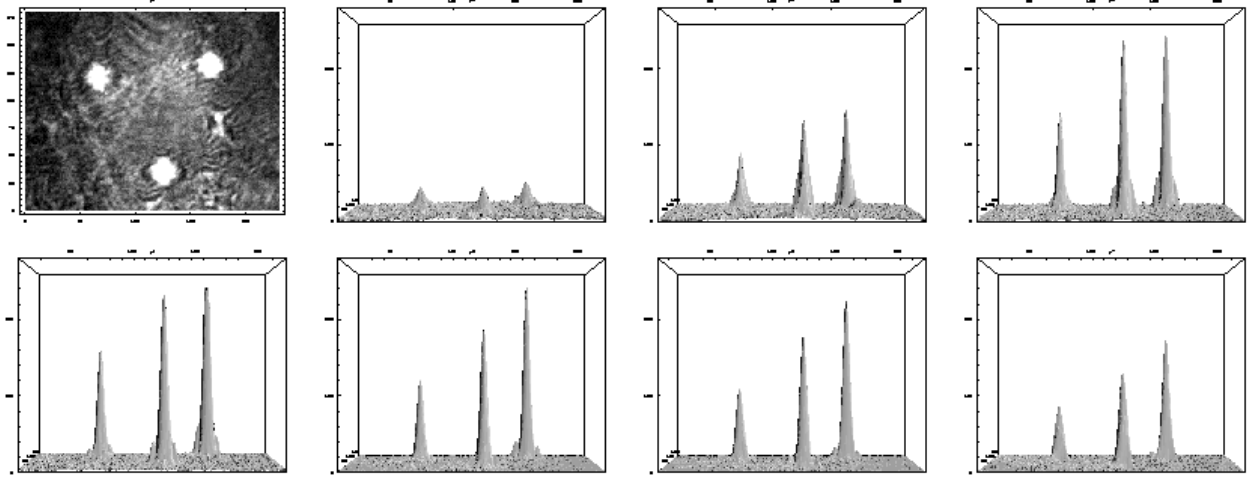


Fig. 5. Multiple-item searching using the triple dot oracle. The upper left panel shows a grey scale image showing the three peaks in white. The remaining seven panels are 3-d plots of the peaks after $\frac{1}{2}$ through $6\frac{1}{2}$ round trips.

plate inside the cavity, each taken in double pass.

The second trace (b) in Fig. 6 is the same as the first, except that now the focus phase plate is positioned as closely as possible to the waist of the beam in the focal plane. Ideally this should give an identical spectrum, apart from an overall phase shift of π . In reality the spectrum looks more messy. This is understandable in view of the difficulty mentioned to mode match the waist in the focal plane to the shape of the phase spot.

Finally, the lower two traces (c) and (d) in Fig. 6 constitute the actual cw experiment. Here the oracle phase spot is placed inside the beam profile. Moreover, instead of measuring the entire power transmitted through the output mirror of the cavity we now image the plane of the output mirror onto the plane of the $150\mu\text{m}$ aperture which is placed near the center of the beam and just before the detector. Trace (c) showing the resonant structure corresponds to the case where the position of the aperture coincides with the position of the solution (the sharp feature associated with the oracle phase spot) in the image on the aperture plane. If the oracle phase spot is slightly moved so that the spike falls just outside the region of the aperture, the featureless trace (d) is measured. The signal to noise ratio of the peaks in the spectrum is at about 20. No vestige of the peaks can be seen just when the peak is moved outside the location of the aperture indicating that the intensity of the solution is at least 20 times higher than the background. The fact that we do not see the

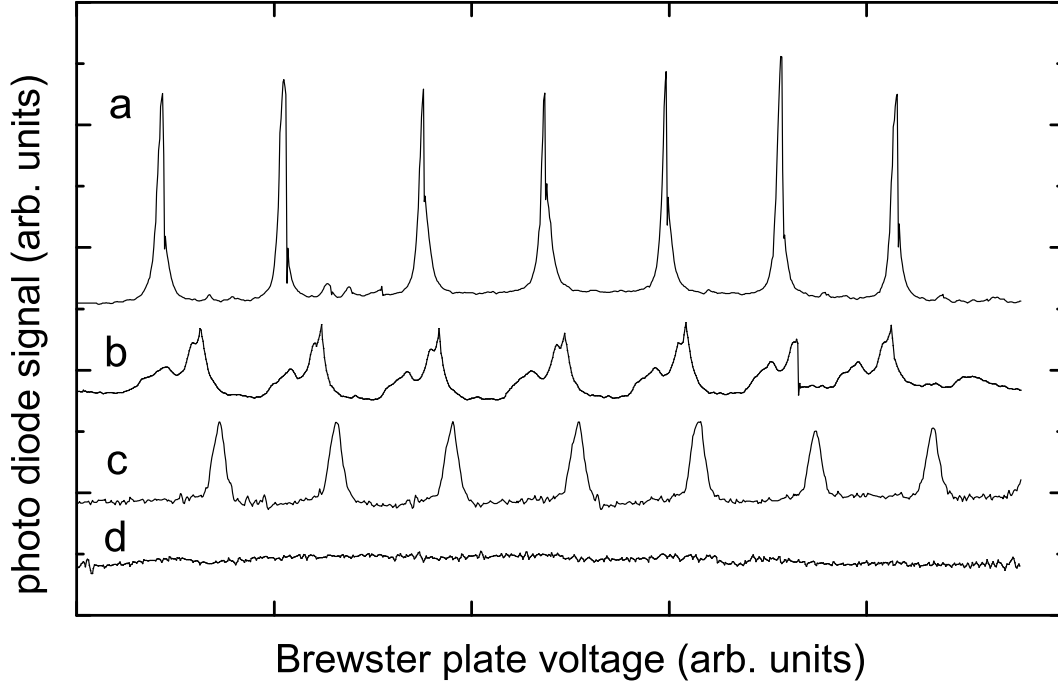


Fig. 6. Photodiode signal taken at the image plane of the output mirror after a scanning cavity. Traces a and b are full images of the output power, taken with and without the focus phase plate. Traces c and d are taken with a $150\mu\text{m}$ aperture in front of the photo diode centered exactly on, and just beside, the position of the solution.

predicted doublet structure in the cavity resonance is due to the low finesse. From Fig. 6d we estimate the value of F to be about 9. This is consistent with about 50% losses per round trip, roughly the same as in the pulsed experiment. As we see from Fig. 2 for such a value of F the power in the peak is reduced by about a factor 20 as compared to the case of high finesse. For $N = 400$ this still gives a peak intensity a factor 20 above background, in excellent agreement with the observation.

Finally we should note that if we integrate the results of Fig. (6) over frequency we still retain a strong amplification of the solution. In other words, the scheme still works with “white light”. In this case the enhancement of the solution is half of the value compared to the resonant monochromatic case. The same is true if we integrate the time domain results over time. This suggests practical applications outside the direct field of quantum

information.

Seen from a different perspective, the system essentially behaves as a phase contrast microscope operated in a multi-pass fashion. The phase difference imparted by the oracle is transformed into an amplitude contrast. Grover's algorithm ensures that this contrast is enhanced by a huge factor. This works for a single search item but also for a multiple item oracle. One could well ask if this scheme could in principle be used to enhance the contrast of an image with an arbitrary phase pattern. At first sight it might seem that the usefulness of Grover's algorithm is rather limited in this case. The reason is that the enhancement of the amplitude of the search items upon iteration only occurs if the phase shift imparted by the oracle items is the same as that of the focus phase plate. On the other hand we may envisage using this feature to our advantage. Grover's algorithm still works if the total phase shift imparted by the oracle and the phase plate are different from π as long as they are equal. If we see our oracle as a mask containing regions that give different phase shifts, we can imagine using a focus phase plate with a variable phase shift to selectively enhance the contrast of specific regions that have just that phase shift. Such a variable-contrast phase plate could possibly be constructed using a liquid crystal device.

6. Conclusion

We have demonstrated that Grover's algorithm can be implemented using a classical optical arrangement relying only on interference and without the need to invoke entanglement. The two dimensional version of the experiment presented here provides a search space of between 400 to 1000 items which would correspond to between 8 and 10 qubits in the quantum version. By exploiting the resonance properties of the cavity and by using monochromatic cw light, we have been able to demonstrate a version of the experiment that is difficult, if not impossible, to implement in the quantum version of the experiment. The transverse beam profile inside the cavity establishes a steady state solution in this case that is a superposition of the input state and the sought solution. The intensity in the sought peak is more than an order of magnitude larger than that obtained in a single pass. Our experiment may have practical applications outside the direct field of quantum information, e.g. by providing new phase contrast imaging methods.

We acknowledge Chris Retif at the Amsterdam nanoCenter for assistance with producing the phase plates used in the experiments. This work is part of the research program of the

Stichting voor Fundamenteel Onderzoek van de Materie (Foundation for the Fundamental Research on Matter) and was made possible by financial support from the Nederlandse Organisatie voor Wetenschappelijk Onderzoek (Netherlands Organization for the Advancement of Research).

References

1. L. K. Grover, Phys. Rev. Lett. **79**, 325 (1997).
2. L. K. Grover, Phys. Rev. Lett. **79**, 4709 (1997).
3. J. A. Jones, M. Mosca, and R. H. Hansen, Nature **393**, 344 (1998).
4. I. L. Chuang, N. Gershenfeld, and M. Kubinec, Phys. Rev. Lett. **80**, 3408 (1998).
5. P. G. Kwiat, J. R. Mitchell, P. D. D. Schwindt, and A. G. White, J. Mod. Opt. **47**, 257 (2000).
6. J. Ahn, T. C. Weinacht, and P. H. Bucksbaum, Science **287**, 463 (2000).
7. C. Dorrer, P. Londero, M. Anderson, S. Wallentowitz, and I. A. Walmsley, in *Proc. CLEO/QELS 2001* (OSA, Washington DC, 2001).
8. N. Bhattacharya, H.B. van Linden van den Heuvell, and R.J.C. Spreeuw, Phys. Rev. Lett. **88** 137901 (2002),
9. G. Puentes, C. La Mela, S. Ledesma, C. Iemmi, J.P. Paz, and M. Saraceno, Phys. Rev. A **69** 042319 (2004).
10. S. Lloyd, Phys. Rev. A **61**, 010301(R) (1999).
11. R. J. C. Spreeuw, Found. Phys. **28**, 361 (1998).
12. R. J. C. Spreeuw, Phys. Rev. A **63**, 062302 (2001).
13. M.A. Nielsen and I.L. Chuang, Quantum Computation and Quantum Information, Cambridge 2000.